

Theory for quenches from ordered states in nonconserved systems

B. Morin, K.R. Elder, and Martin Grant

Department of Physics, McGill University, Rutherford Building, 3600 University Street, Montréal, Québec, Canada H3A 2T8
(Received 12 August 1992)

Motivated by recent experiments, a theory for the dynamics that follow a quench from an ordered state to both ordered and disordered regions is presented for systems with a nonconserved order parameter. For quenches below the anneal temperature, an initial growth of fluctuations is followed by a decay to the equilibrium values. For sufficiently low temperatures a temporary instability to phase separation occurs giving rise to an effective spinodal curve. Quenches to the disordered phase are found to involve nonexponential relaxation in the early stages. Analytic expressions are obtained for the dynamic structure factor for all these situations and their relevance to recent experiments is discussed.

I. INTRODUCTION

Quenches of systems with a nonconserved order parameter have been studied intensively.¹⁻¹⁶ These processes describe order-disorder transitions in alloys and paramagnetic-antiferromagnetic transitions in Ising-like systems. In a typical experiment, a system is prepared in the disordered or high-temperature phase and rapidly quenched to a lower temperature where an ordered phase is preferred. The dynamics that follow the quench involve the creation of ordered domains that coarsen or enlarge as time evolves. The late stage dynamics of these transformations is well understood and is controlled by the motion of domain walls or antiphase boundaries. Allen and Cahn² have described domain growth by assuming that the antiphase boundaries propagate as solitary waves. They found a constant velocity proportional to the mean curvature from which follows a $t^{1/2}$ growth law for the average domain size. There have been many other theoretical approaches to this problem^{4,5,7,16} which yield more detailed information, but essentially recover the fundamental $t^{1/2}$ growth law. In addition there have been extensive numerical^{8,9,12,14} and experimental^{1,2,10,11,13} verifications of this result. In this paper we focus on quenches for which the initial state is in the ordered region. This work was motivated by recent *in situ* time resolved x-ray scattering experiments of Park *et al.*¹ on the ordering dynamics of Fe₃Al in the DO₃ phase.

These experiments display intriguing behavior, somewhat analogous to the early stages of growth for a quench from the disordered to the ordered regime. Upon a quench from an anneal temperature of T_a to a temperature of T_Q (such that $T_c > T_a > T_Q$, where T_c is the critical temperature) the Bragg peak associated with the sublattice concentration (or DO₃ phase) always relaxes exponentially to a higher value, indicating no phase separation. In contrast, the x-ray intensity associated with the short-range order (or fluctuations about the ordered phase) appears to sharpen at early times. In quenches from the disordered regime to the ordered region this sharpening is associated with the creation and growth of

domains. The results of our study herein indicate that a sharpening of the x-ray intensity can occur due to a subtle coupling between long- and short-range order, without the creation of domain walls.

Our work focuses on a simple model of this process known as model *A* in the Halperin and Hohenberg¹⁷ classification scheme. Model *A* is a nonlinear Langevin model that describes the dynamics of a nonconserved field (ψ), which would correspond to the sublattice concentration in order-disorder transitions. Although model *A* is highly nonlinear, analytic expressions are obtained for the dynamic structure factor (which is equivalent to the x ray intensity measured in experiment) by decoupling the growth of the mean value of the ordering field (ψ_0) from fluctuations ($\delta\psi$) about it. This decoupling leads to a nonlinear, but spatially independent equation for ψ_0 and a linear equation of motion for $\delta\psi$, both of which can be solved exactly. In the next section model *A* is presented and the initial prequench state is described in terms of quantities measured in x-ray scattering experiments. The following section provides the details of the approximation scheme outlined above and discusses the results of these approximations. Finally a summary of results is given and their relevance to experiment is discussed in the last section.

II. MODEL EQUATIONS

The partition function contains all the information relevant to the equilibrium properties of statistical systems. For a system with a single order parameter, the partition function takes the form

$$\mathcal{Z} = \int \{\mathcal{D}\psi\} e^{-H[\psi]/k_B T}. \quad (1)$$

$H[\psi]$, the Hamiltonian, can be generally written,

$$H[\psi] = \int d\mathbf{x} \left(\frac{\kappa}{2} |\nabla\psi|^2 + \mathcal{V} \right). \quad (2)$$

Here it is assumed the potential density \mathcal{V} is a function

of ψ only. The nonequilibrium behavior of this system is given by a Langevin equation, which assumes the dynamics of ψ are governed by the minimization of $H[\psi]$. The Langevin equation is a classical equation of motion for the field ψ to which a random noise term with a well defined distribution is added, to take into account thermal fluctuations. It is written as

$$\begin{aligned} \frac{\partial \psi(\mathbf{x}, t)}{\partial t} &= -\Gamma \frac{\delta H[\psi]}{\delta \psi(\mathbf{x}, t)} + \eta(\mathbf{x}, t) \\ &= \Gamma \left(\kappa \nabla^2 \psi(\mathbf{x}, t) - \frac{\partial \mathcal{V}(\psi(\mathbf{x}, t))}{\partial \psi(\mathbf{x}, t)} \right) + \eta(\mathbf{x}, t). \end{aligned} \quad (3)$$

$\eta(\mathbf{x}, t)$ is a scalar field associated with the thermal fluctuations and its distribution can be defined by its moments. We will use the usual Gaussian distribution which is completely specified by

$$\begin{aligned} \langle \eta(\mathbf{x}, t) \rangle &= 0, \\ \langle \eta(\mathbf{x}, t) \eta(\mathbf{x}', t') \rangle &= 2\Gamma k_B T \delta(\mathbf{x} - \mathbf{x}') \delta(t - t'). \end{aligned} \quad (4)$$

In the vicinity of T_c , the equilibrium properties of systems undergoing a second-order phase transition are well described by an effective Hamiltonian density of the form, $H[\psi] = \kappa |\nabla \psi|^2 / 2 - r \psi^2 / 2 + s \psi^4 / 4$, where $\psi(\mathbf{x})$ is a scalar field which, when averaged over thermal fluctuations, $\langle \psi(\mathbf{x}) \rangle$, plays the role of the order parameter. When there is no external field present, as is the case here, the Hamiltonian is symmetric under the parity transformation $\psi(\mathbf{x}) \rightarrow -\psi(\mathbf{x})$. For $r < 0$ the order parameter is zero and symmetric: $\langle \psi(\mathbf{x}) \rangle = \langle -\psi(\mathbf{x}) \rangle = 0$. This characterizes the disordered phase. When $r > 0$ the order parameter is nonzero and not symmetric: $\langle \psi(\mathbf{x}) \rangle \neq 0$, $\langle \psi(\mathbf{x}) \rangle \neq \langle -\psi(\mathbf{x}) \rangle$. This shows spontaneous symmetry breakdown and characterizes the ordered phase. We shall make use of this form, although we will consider temperatures T_a and T_Q sufficiently far from T_c that we are not in the critical regime.

The reordering that occurs when a system in its ordered state undergoes a rapid change in temperature (be it to higher or lower temperatures) will be investigated using the ψ^4 Hamiltonian density given above. For such purposes it is convenient to employ dimensionless variables, by rescaling space, time, ψ , and η in the following manner:

$$\tau = \Gamma_Q |r_Q| t, \quad \boldsymbol{\rho} = \sqrt{|r_Q| / \kappa_Q} \mathbf{x}, \quad \phi = \sqrt{s_Q / |r_Q|} \psi, \quad (5)$$

$$\zeta = \sqrt{s_Q / |r_Q|} / (\Gamma_Q |r_Q|) \eta,$$

where the subscript Q refers to the quenched state. In these variables, for the ψ^4 model, Eq. (3) becomes

$$\frac{\partial \phi(\boldsymbol{\rho}, \tau)}{\partial \tau} = (\pm 1 + \nabla_{\boldsymbol{\rho}}^2) \phi(\boldsymbol{\rho}, \tau) - \phi^3(\boldsymbol{\rho}, \tau) + \zeta(\boldsymbol{\rho}, \tau), \quad (6)$$

where $\langle \zeta(\boldsymbol{\rho}, \tau) \zeta(\boldsymbol{\rho}', \tau') \rangle = 2\varepsilon_Q \delta(\boldsymbol{\rho} - \boldsymbol{\rho}') \delta(\tau - \tau')$ and $\varepsilon_Q = k_B T_Q s_Q / |r_Q|^2 (|r_Q| / \kappa_Q)^{d/2}$. The plus and minus

sign corresponds to quenches below and above T_c , respectively. The phenomenological constants can be related to the susceptibility (χ), the saturation value of ψ (ψ_∞), and the correlation length (ζ), i.e.,

$$\chi_Q = \frac{1}{a_0^d} \frac{k_B T_Q}{|r_Q|}, \quad \psi_\infty^2 = \psi_Q^2 = \frac{|r_Q|}{s_Q}, \quad \xi_Q^2 = \frac{\kappa_Q}{|r_Q|}, \quad (7)$$

where a_0 stands for the lattice constant. Hence, the noise strength can be written

$$\varepsilon_Q = \frac{\chi_Q}{\psi_Q^2} \left(\frac{a_0}{\xi_Q} \right)^d. \quad (8)$$

To solve Eq. (6) we split ϕ into two parts, i.e.,

$$\phi(\boldsymbol{\rho}, \tau) = \phi_0(\tau) + \delta\phi(\boldsymbol{\rho}, \tau). \quad (9)$$

The first term is the average value of the field, $\phi_0(\tau) = \langle \phi(\boldsymbol{\rho}, \tau) \rangle$, and is spatially uniform while $\delta\phi(\boldsymbol{\rho}, \tau)$ represents fluctuations about this average value. In what follows we assume that $\delta\phi$ is a small parameter so that its equation of motion can be linearized, the validity of which will be discussed later. Let us now consider a quench from an anneal temperature $T_a < T_c$ to a temperature $T_Q < T_c$. The theory can be formulated using three parameters that correspond to ratios of measurable physical quantities. One is the ratio of the square of the saturation value at the initial temperature T_a , to its value at the final temperature T_Q , which is equivalent to the ratio of the Bragg peaks associated with the long-range order, i.e.,

$$R_I = \frac{\psi_a^2}{\psi_Q^2} = \frac{I_a^B}{I_Q^B}, \quad (10)$$

where I_a^B and I_Q^B correspond to the intensity of the Bragg peak in the anneal and quench states, respectively. The ratio of the susceptibilities, R_χ can be estimated by subtracting the Bragg intensity from the total scattering pattern. What is left corresponds to the structure factor of the fluctuations around the ordered state, normally referred to as the short-range order and usually assumed to be a Lorentzian of the form,

$$S(q) = \frac{I^D}{q^2 \xi^2 + 2}. \quad (11)$$

where $S(q, \tau) \equiv \langle |\delta\phi(q, \tau)|^2 \rangle / [(2\pi)^d \delta(\mathbf{q} + \mathbf{q}')]$. The ratio R_χ can thus be related to an experimental quantity in the following way:

$$R_\chi = \frac{\chi_a}{\chi_Q} = \frac{I_a^D}{I_Q^D}. \quad (12)$$

The last parameter is the ratio of the square of the correlation length. It is written as

$$R_\xi = \frac{\xi_a^2}{\xi_Q^2} = \frac{\kappa_a |r_Q|}{r_a \kappa_Q}. \quad (13)$$

The initial and final structure factors then take the form

$$\langle |\phi(q, \tau = 0_-)|^2 \rangle = R_I (2\pi)^d \delta(\mathbf{q}) + \varepsilon_Q R_\chi / (q^2 R_\xi + 2), \quad (14)$$

$$\langle |\phi(q, \tau = \infty)|^2 \rangle = (2\pi)^d \delta(\mathbf{q}) + \varepsilon_Q / (q^2 + 2).$$

In the dimensionless units defined by Eq. (5) the correlation length is $1/\sqrt{2}$. For a process where $T_Q > T_c$, $\phi_0(\tau \rightarrow \infty) = 0$ and the equilibrium structure factor is given by

$$\langle |\phi(q, \tau = \infty)|^2 \rangle = \varepsilon_Q / (q^2 + 1). \quad (15)$$

III. APPROXIMATE SOLUTION OF MODEL EQUATIONS

To analyze the reordering that takes place when the system is quenched from an anneal temperature $T_a < T_c$ to a temperature T_Q , it is assumed that the equation of motion for ϕ_0 can be decoupled from that for $\delta\phi$. For a general Hamiltonian specified by Eq. (2), the equations of motion for the average saturation value and for the structure factor of the fluctuations respectively, are

$$\frac{\partial \psi_0(t)}{\partial t} = -\Gamma \frac{\partial \mathcal{V}[\psi_0(t)]}{\partial \psi_0(t)}, \quad (16)$$

$$\frac{\partial S(q, t)}{\partial t} = -2\Gamma \left(\frac{\kappa}{2} q^2 + \frac{\partial^2 \mathcal{V}[\psi_0(t)]}{\partial \psi_0^2(t)} \right) S(q, t) + 2\Gamma k_B T.$$

Here all nonlinear contributions to the equation of motion for $\delta\phi$ have been dropped. In rescaled units the ψ^4 model then becomes

$$\frac{\partial \phi_0(\tau)}{\partial \tau} = \pm \phi_0(\tau) - \phi_0^3(\tau), \quad (17)$$

$$\frac{\partial S(q, \tau)}{\partial \tau} = 2[\pm 1 - q^2 - 3\phi_0^2(\tau)]S(q, \tau) + 2\varepsilon_Q. \quad (18)$$

As before, the plus and minus signs correspond to $T_Q < T_c$ and $T_Q > T_c$, respectively. Solving for $\phi_0(\tau)$ gives the time evolution of the Bragg intensity, i.e.,

$$\phi_0^2(\tau) = \frac{I^B(\tau)}{I_Q^B} = \frac{e^{\pm 2\tau} R_I}{1 \pm (e^{\pm 2\tau} - 1) R_I}. \quad (19)$$

As mentioned earlier, for a quench within the disordered region, R_I is the ratio of the Bragg intensities, I_a^B/I_Q^B . When the system is heated up to a temperature above T_c , this quantity does not clearly correspond to any measurable quantity. Far above T_c , the Hamiltonian can usually be well approximated by a ψ^2 model, since higher orders are only important when the fluctuations are large. Nevertheless, these higher-order terms do play a role when the prequench state has an average value that is large, as is the case considered here. For estimation purposes we assume that s is approximately constant below as well as above T_c .

Regardless of the precise value of R_I , Eq. (19) shows a relaxation from an initial state R_I to the final state which is equal to 1 when $T_Q < T_c$ and 0 when $T_Q > T_c$. $\delta\phi$ shows a much richer behavior. This is due to the

time dependence of the dispersion relation [i.e., $\omega(q, \tau)$, where $S(q, \tau) = e^{\omega(q, \tau)t} S(q, 0)$], which is dictated by the reequilibration of the long-range order. The dispersion relation is

$$\omega(q, \tau) = \pm 1 - q^2 - \frac{3}{\tau} \int_0^\tau d\tau' \phi_0^2(\tau'), \quad (20)$$

which defines a dynamic spinodal at

$$\omega(0, 0) = 0, \quad \rightarrow \quad \phi_{\text{sp}} = \sqrt{\frac{I_a^B}{I_Q^B}} = \frac{1}{\sqrt{3}}. \quad (21)$$

This effective spinodal defines the initial stability of the fluctuations, such that for $\phi_0(0) < \phi_{\text{sp}}$ and $\phi_0(0) > \phi_{\text{sp}}$, $\delta\phi$ will grow or decay, respectively. This is analogous to the spinodal line defined in spinodal decomposition, except that it only applies to the initial stages of growth. Figures 1(a) and 1(b), respectively, show the dispersion relation at various times for a quench above and below the spinodal curve. A linear instability is seen at early times for quenches below the spinodal line [Fig. 1(b)]. Nevertheless, $\delta\phi$ is always linearly stable at late times.

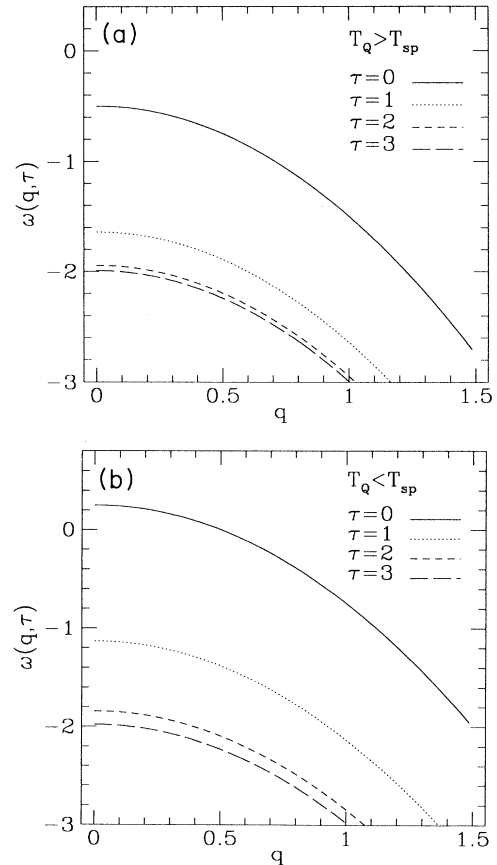


FIG. 1. The dispersion relationship is shown at various times for $T_Q/T_c = 0.8$ and $T_Q/T_c = 0.6$ in Figs. (a) and (b), respectively with $T_a/T_c = 0.9$. In both figures the curves from top to bottom correspond to $\tau = 0, 1, 2,$ and 3 .

The linear approximation for $\delta\phi$ would not be appropriate if $I^D(0)/I^B(0) \approx 1$, since this could lead to the creations of domain. However, if $I^D(0)/I^B(0) \ll 1$, the time period over which $\delta\phi$ is unstable is not sufficient to create domains. The reason for this is that the maximum rate of growth of $\delta\phi$ is less than the rate of growth of ϕ_0 . Consequently if $I^D(0)/I^B(0) \ll 1$, then $I^D(\tau)/I^B(\tau) \ll 1$ for

all $\tau > 0$. For quenches above T_c , $\delta\phi$ is always linearly stable and thus the linearization scheme is appropriate. The theory is not valid in the vicinity of T_c where non-linear terms are known to play a crucial role in both equilibrium and nonequilibrium phenomena.

The structure factor for $\delta\phi$ can be obtained from Eq. (18) and is

$$S(q, \tau) = \frac{\varepsilon_Q}{[1 \pm (e^{\pm 2\tau} - 1)R_I]^3} \left[(1 \mp R_I)^3 \left(\frac{1 - e^{-(q^2 \mp 1)2\tau}}{q^2 \mp 1} \right) \pm 3(1 \mp R_I)^2 R_I e^{\pm 2\tau} \left(\frac{1 - e^{-2q^2\tau}}{q^2} \right) \right. \\ \left. + 3(1 \mp R_I)(R_I e^{\pm 2\tau})^2 \left(\frac{1 - e^{-(q^2 \pm 1)2\tau}}{q^2 \pm 1} \right) \right. \\ \left. \pm (R_I e^{\pm 2\tau})^3 \left(\frac{1 - e^{-(q^2 \pm 2)2\tau}}{q^2 \pm 2} \right) + R_\chi \frac{e^{-(q^2 \mp 1)2\tau}}{q^2 R_\xi + 2} \right]. \quad (22)$$

The first four terms of this expression correspond to the growth of the new fluctuations. The last term describes the initial fluctuations, which go to zero in the infinite time limit. This form ensures that the structure factor gives the correct final distribution both for quenches within the ordered region (upper sign), and for quenches up to the disordered region (lower sign).

IV. RESULTS

Equations (19) and (22) are the main results of this work and describe the dynamics of the long- and short-range order, respectively. To elucidate the behavior of these equations it is necessary to determine approximate values for the three ratios, R_I , R_χ , and R_ξ . To do so, mean-field results are used, since mean-field theory works quite well for the quenches considered here (note for quenches near T_c the linearization for $\delta\phi$ breaks down).

The mean-field values are

$$R_I = \frac{1 - T'_a}{|1 - T'_Q|}, \quad R_\chi = \frac{T'_a}{T'_Q} \frac{|1 - T'_Q|}{1 - T'_a}, \quad R_\xi = \frac{|1 - T'_Q|}{1 - T'_a}, \quad (23)$$

where the temperatures have been scaled by the critical temperature, e.g., $T' = T/T_c$. The spinodal temperature T'_{sp} is then $T'_{sp} = 3T'_a - 2$. For illustrative purposes we consider $T'_a = 0.9$, which gives, $T'_{sp} = 0.7$. These quenches are schematically represented in Fig. 2 (which also includes quenches to above T_c). In Figs. 3, 4, and 5 the Bragg intensity [i.e., $\phi(\tau)^2$], $S(k=0, \tau)$ and $\xi(\tau)$ are shown for quenches below T_c , respectively. $\xi(\tau)$ is defined as the half-width at half-maximum of $S(k, \tau)$. It should be noted that $S(k, \tau)$ fits a Lorentzian well at all times. In these figures three temperatures are considered, one above T'_a (i.e., $T'_Q = 0.95$) one below T'_a but above the spinodal (i.e., $T'_Q = 0.8$) and one below the

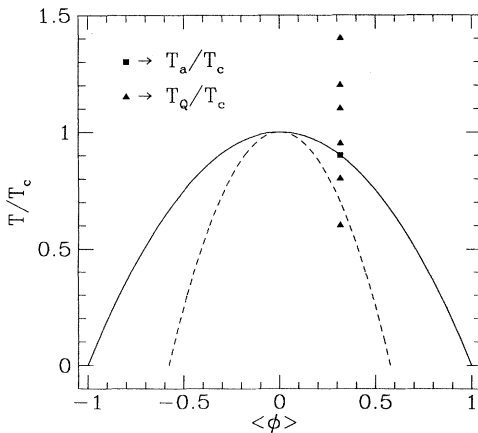


FIG. 2. Plot of the coexistence curve (solid line) and of the spinodal curve (dotted line) defined in Eq. (21). The square and triangles correspond to the anneal and quench temperatures considered in latter plots, respectively. For all subsequent plots, the anneal temperature is $T'_a = 0.9$.

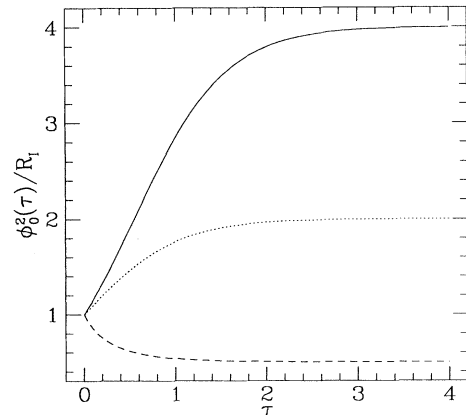


FIG. 3. The Bragg peak is plotted as a function of time. The solid, dotted, and dashed lines correspond to quenches to temperatures of $T'_Q = 0.6, 0.8$, and 0.95 , respectively. The effective spinodal temperature is at $T'_{sp} = 0.7$.

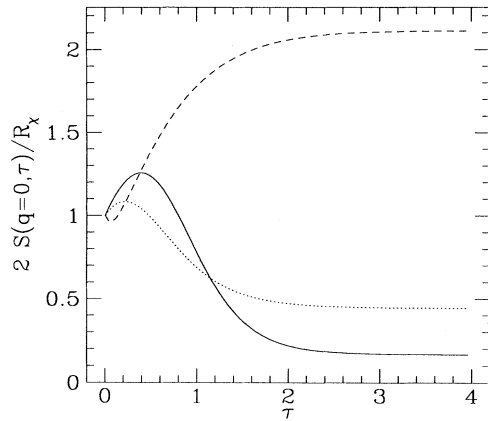


FIG. 4. $S(k = 0, \tau)$ is shown as a function of time for several quench temperatures. The line types are the same as in Fig. 3.

spinodal (i.e., $T'_Q = 0.6$). In all these figures, the quantities plotted are rescaled so that at $\tau = 0$ they agree. For these three quenches, the Bragg intensity, shown in Fig. (3), monotonically relaxes to its equilibrium value consistent with the experiment of Park *et al.*¹ Figures 4 and 5 indicate that the dynamics of $S(0, \tau)$ and $\xi(\tau)$ are qualitatively different for quenches above and below T_a . For quenches below T_a both quantities initially increase before decreasing to the final equilibrium values, while for quenches above T_a there is an initial decrease before a final rise to the equilibrium values. The reason for the complex nonexponential behavior is due to the changing value of ϕ_0 or $\omega(q, \tau)$. In essence, at early times the average value of ϕ has not reached its equilibrium value and consequently $\delta\phi$ is relaxing to a state that is not commensurate with the infinite time solution. It is interesting to note that the spinodal does not seem to play an important role, such that quenches above and below the spinodal are qualitatively similar.

Similar plots are shown for quenches above T_c in

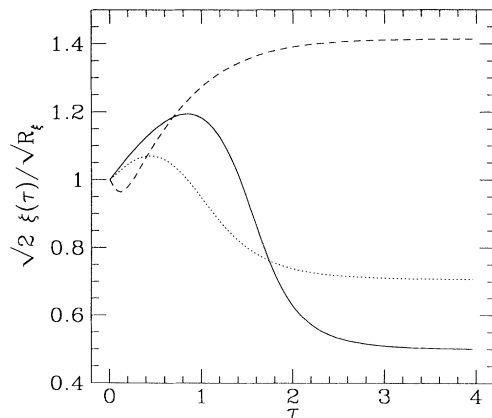


FIG. 5. The evolution of the correlation length is shown as a function of time for several quench temperatures. The line types correspond to the same temperatures as in Fig. 3.

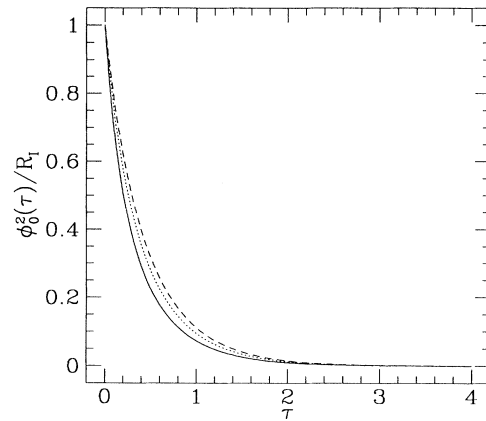


FIG. 6. The relaxation of the Bragg peak for quenches above T_c is shown in this figure. The solid, dotted, and dashed lines correspond to quench temperatures of $T'_Q = 1.1$, 1.2, and 1.3.

Figs. 6–8 for the Bragg intensity, $S(0, \tau)$, and $\xi(\tau)$, respectively. The temperatures considered are $T'_Q = 1.1$, $T'_Q = 1.2$, and $T'_Q = 1.4$ as shown in Fig. 2. Contrary to quenches below T_c , the Bragg intensity relaxes to zero, which means that the order parameter is zero and the symmetry of the disordered phase is restored. The diffuse peak intensity and the correlation length evolve to their equilibrium value in a way similar to quenches above the anneal temperature but below T_c . The sudden change in temperature (which corresponds to an abrupt variation of the parameters) creates a far from equilibrium state into which $S(k, \tau)$ tries to relax. Note that this nontrivial relaxation of the diffuse intensity peak and of the correlation length depends crucially on the nonlinear treatment of the average saturation value even though we are quenching up to the disordered phase. These events can also be seen experimentally, although the decoupling between the Bragg intensity and the diffuse intensity mentioned before will be much harder to perform correctly;

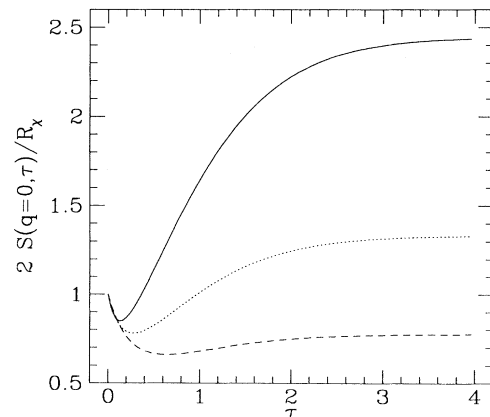


FIG. 7. $S(k = 0, \tau)$ is shown as a function of scaled time for quenches into the disordered phases. The line types correspond to those given in Fig. 6.

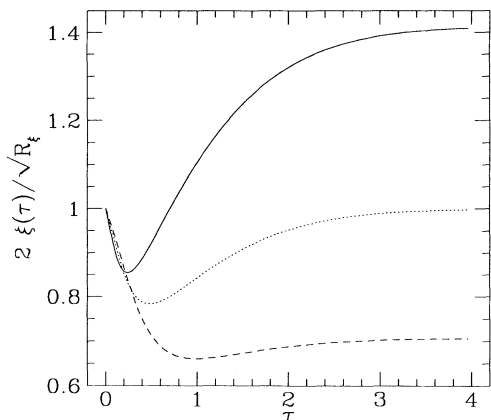


FIG. 8. The evolution of the correlation length is plotted as a function of time. The line types correspond to those given in Fig. 6.

as the Bragg intensity goes to zero, it will be confounded with the diffuse peak.

V. CONCLUSION

We have outlined a theory for the relaxational dynamics of a quenched nonconserved system with its initial state in the ordered region. This theory predicts interesting behavior which is consistent with recent experiments

on Fe_3Al in the DO_3 phase by Park *et al.*¹ The behavior of the diffuse peak (associated with the short-range order) is strongly correlated with the dynamics of the Bragg intensity (associated with the long-range order). In essence the short-range order fluctuations attempt to relax to a value consistent with the average value of the order parameter which is time dependent. This complex process leads to nontrivial dynamical behavior of the short-range order peak. In summary we believe that the apparent sharpening of the short-range order peak seen in the experiments of Park *et al.*¹ is consistent with our results and is not necessarily due to the creation of anti-phase boundaries. A direct comparison with experiment is unfortunately quite difficult, due to the dependence of $S(q, \tau)$ on $\phi(\tau)$. The solution for $\phi(\tau)$ given in Eq. (19) depends on the specific form of free energy used (e.g., a ϕ^4 free energy used here). It may be that for quantitative comparison with experiment, a more realistic free energy must be selected.

ACKNOWLEDGMENTS

The authors would like to thank Karl F. Ludwig, Byungwoo Park, G. Brian Stephenson, and Mark Sutton for useful discussions. The research was kindly supported by the Natural Sciences and Engineering Council of Canada and by les Fonds pour la Formation de Chercheurs et l'Aide à la Recherche de la Province de Québec.

¹B. Park, G.B. Stephenson, K.F. Ludwig, and S. M. Allen, *Mat. Res. Soc. Symp. Proc.* **205**, 119 (1992); *Phys. Rev. Lett.* **68**, 1742 (1992).

²S.M. Allen and J.W. Cahn, *Acta Met.* **23**, 1017 (1975); **27**, 1085 (1975); **24**, 425 (1976).

³J.D. Gunton and M. Droz, *Introduction to the Theory of Metastable and Unstable States* (Springer-Verlag, Berlin, 1983).

⁴K. Kawasaki, M.C. Yalabik, and J.D. Gunton, *Phys. Rev. A* **17**, 455 (1978).

⁵K.R. Elder, B. Morin, M. Grant, and R.C. Desai, *Phys. Rev. B* **44**, 6673 (1991).

⁶R.K.P. Zia, R. Bausch, H.K. Janssen, and V. Dohm, *Mod. Phys. Lett. B* **2**, 961 (1988).

⁷T. Ohta, D. Jasnow, and K. Kawasaki, *Phys. Rev. Lett.* **49**, 1223 (1982); T. Ohta, *Ann. Phys. (N.Y.)* **158**, 31 (1984).

⁸Y. Oono and S. Puri, *Phys. Rev. Lett.* **58**, 836 (1987); *Phys. Rev. A* **38**, 1542 (1988); *Mod. Phys. Lett. B* **2**, 861 (1988).

⁹A. Sadiq and K. Binder, *J. Stat. Phys.* **35**, 517 (1984).

¹⁰S.M.L. Sastry and H.A. Lipsitt, *Metal. Trans.* **8A**, 1543 (1977).

¹¹M. Seki and D.E. Mikkola, *Metal. Trans.* **2**, 1635 (1971); C.L. Rase and D.E. Mikkola, *ibid.* **6A**, 2267 (1975).

¹²C. Roland and M. Grant, *Phys. Rev. B* **41**, 4663 (1990).

¹³S.E. Nagler, R.F. Shannon, Jr., C.R. Harkless, M.A. Singh, and R.M. Nicklow, *Phys. Rev. Lett.* **61**, 718 (1988).

¹⁴M. Laradji, M. Grant, M.J. Zuckermann, and W. Klein, *Phys. Rev. B* **41**, 4646 (1990).

¹⁵P.S. Sahni, J.D. Gunton, S.L. Katz, and R.H. Timpe, *Phys. Rev. Lett.* **43**, 369 (1980).

¹⁶G.F. Mazenko, O.T. Valls, and M. Zannetti, *Phys. Rev. B* **38**, 520 (1988); G.F. Mazenko, *Phys. Rev. Lett.* **63**, 1605 (1989).

¹⁷P.C. Hohenberg and B.I. Halperin, *Rev. Mod. Phys.* **49**, 435 (1977).